ASTRONOMY AND ASTROPHYSICS LIBRARY

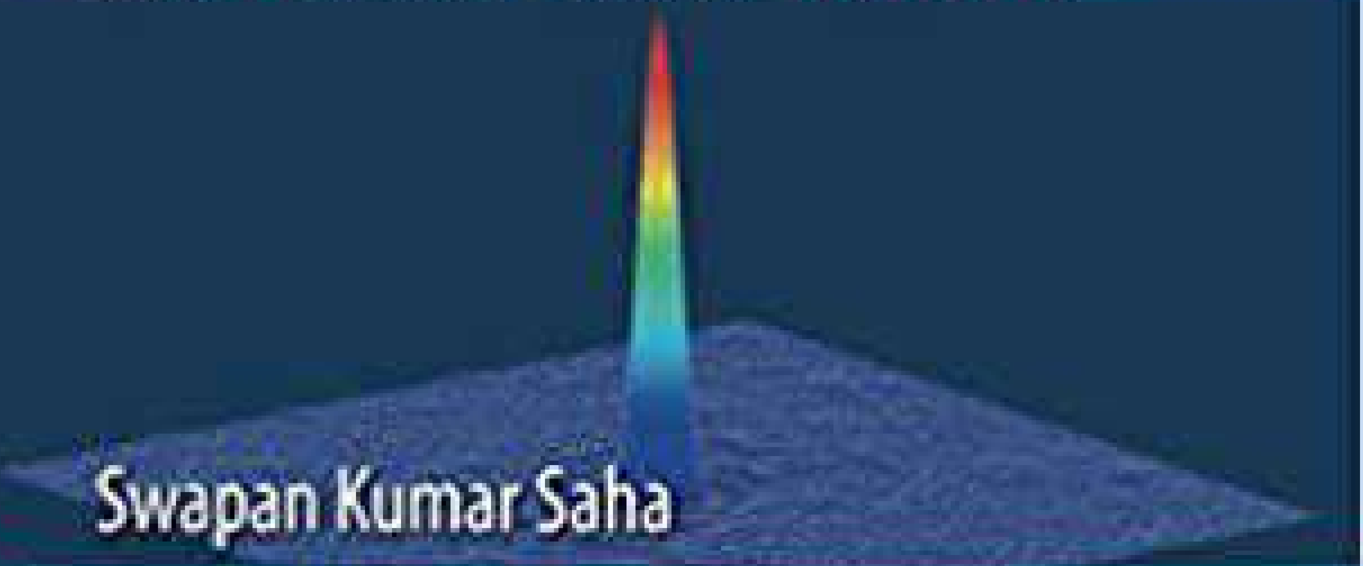

Swapan Kumar Saha

Aperture Synthesis

Methods and Applications to Optical Astronomy

A&A LIBRARY

Springer

LIBRARY

ASTRONOMY AND ASTROPHYSICS LIBRARY

For further volumes:
http://www.springer.com/series/848

S.K. Saha

Aperture Synthesis

Methods and Applications to Optical Astronomy

Springer

Swapan Kumar Saha
Indian Institute of Astrophysics
Sarjapur Road
560034 Bangalore
IInd Block, Koramangala
India
sks@iiap.res.in

ISSN 0941-7834
ISBN 978-1-4419-5709-2 e-ISBN 978-1-4419-5710-8
DOI 10.1007/978-1-4419-5710-8
Springer New York Dordrecht Heidelberg London

Library of Congress Control Number: 2010938735

Printed on acid-free paper

Springer is part of Springer Science+Business Media (www.springer.com)

To my children, Snigdha and Saurabh

Preface

The angular resolution of a single aperture (telescope) is inadequate to measure the brightness distribution across most stellar sources and many other objects of astrophysical importance. A major advance involves the transition from observations with a single telescope to a diluted array of two or more telescopes separated by more than their own sizes, mimicking a wide aperture, having a diameter about the size of the largest separation. Such a technique, called aperture synthesis, provides greater resolution of images than is possible with a single member of the array.

Implementation of interferometry in optical astronomy began more than a century ago with the work of Fizeau (1868). Michelson and Pease (1921) measured successfully the angular diameter of Betelgeuse (α Orionis), using an interferometer based on two flat mirrors, which allowed them to measure the fringe visibility in the interference pattern formed by starlight at the detector plane. Later, Hanbury Brown and Twiss (1954) developed the intensity interferometry (see Sect. 3.3). Unlike Michelson (amplitude) interferometry, this does not rely on actual light interference. Instead, the mutual degree of coherence is obtained from the measurement of the degree of correlation between the intensity fluctuation of the signals recorded with a quadratic detector at two different telescopes. It measures the second-order spatial coherance, where the phase of the signals in separate telescopes was not required to be maintained. However, it ended with the Narrabri intensity interferometer (Hanbury Brown 1974) that was used to measure the diameter of bright stars and the orbit of binaries and was the first to measure the limb-darkening of a star other than the Sun. The survey of stellar diameters by means of this instrument serves as a resource for the effective temperature scale of main-sequence stars. Important results were obtained for the spectroscopic and eclipsing binaries as well.

Obtaining a diffraction-limited image of celestial bodies was one of the major problems faced by the optical astronomers in the past. This is mainly due to the image degradation at optical wavelengths produced by the atmospheric turbulence. Labeyrie (1970) developed speckle interferometry as one way to overcome the degradation due to atmospheric turbulence. Then technological advances overcame many of the problems encountered by Michelson and Pease (1921) allowing further development of phase-preserving optical interferometry, more nearly analogous to radio interferometry. Labeyrie (1975) developed a long baseline interferometer with two small optical telescopes and resolved several stars. This technique depends on the visibility of fringes produced by the amplitude interferences formed by the light collected by two telescopes allowing the measurement of stars much fainter than was possible with intensity interferometry using the same size telescopes.

Following the publication of the article entitled, 'Modern Optical Astronomy: Technology and Impact of Interferometry – Swapan K Saha, 2002, Reviews of Modern Physics, **74**, 551–600,' several astronomers, particularly M. K. Das Gupta, who along with R. C. Jennison and R. Hanbury Brown developed intensity interferometry in radio wavelengths, had requested me to write a monograph, for which I am indebted to. In fact, I had the opportunity to be associated with him during graduate school days and discussed at length on this topic. This monograph, a sequel to my earlier book entitled, 'Diffraction-limited Imaging with Large and Moderate Telescopes', 2007, World-Scientific, is a dossier of knowledge for every graduate student and researcher, who intend to embark on a field dedicated to the long baseline aperture synthesis. I have attempted to make this book self-contained by incorporating more than one hundred and fifty illustrations and tens of footnotes. This monograph addresses the basic principles of interferometric techniques, the current trend, motivation, methods, and path to future promise of true interferometry at optical and infrared wavelengths. Since the basic principle of aperture synthesis imaging in optical astronomy using interferometry is Fourier Optics, this topic along with several fundamental equations is also highlighted in the appendices.

The progress in the field of radio interferometry is exemplary. The success is primarily because of the possibility to preserve phase information for widely separated dishes by using very accurate clocks and time markers in the data streams. Though the principles of optical interferometry are essentially identical to those at radio wavelengths, accurate measurements are more difficult to make: (i) the irregularities in the Earth's atmosphere introduce variations in the path length that are large compared to the wavelength; (ii) it is difficult to achieve the required mechanical stability of the telescopes to obtain interference fringes at a wavelength of the order of 500 nm. The calibration of the instrumental phase is a formidable task; and (iii) the division of the photons incident on each telescope in an array of optical telescopes to estimate the mutual coherence function or the complex visibility over the different possible baselines in the array leads to serious signal-to-noise problems. Despite the differences in technology between radio and optical interferometers, a common characterization of source properties, such as source visibility is adequate to provide a qualitative and quantitative description of the response of a long baseline interferometer.

Optical interferometry is generally performed within the standard atmospheric spectral windows. It requires several optical functions such as spatial filtering, which allows determination of the Fourier transform of the brightness distribution at the spatial frequencies, photometric calibration, polarization control etc., but the practical limitations imposed on these measurements are severe. An instrument of this nature needs extreme accuracies to meet the demands of maintaining the optical pathlengths within the interferometer, constant to a fraction of a wavelength of light, which constrained Long Baseline Optical Interferometers (LBOI) to smaller baselines (∼100 m); mostly they operate at longer wavelengths (in the near- and mid-IR bands). The practical considerations regarding extraction of the Fourier components became important to look at. The first chapter lays the foundation of the mathematical framework that is required to understand the theoretical basis for Fourier Optics, imaging systems, while the second and third chapters address the fundamentals of optical interferometry and its applications.

Speckle interferometry (see Sect. 4.2), a post-processing technique, has successfully uncovered details in the morphology of a range of astronomical objects, including the Sun, planets, asteroids, cool giants and supergiants. Fueled by the rapid advancement of technology such as computational, fabrication, and characterization, development on real time corrections of the atmospheric turbulence, called ‘Adaptive Optics’ (AO), has given a new dimension in this field (see Sect. 4.3). Combining with LBOI, it offers the best of both approaches and shows great promise for applications such as the search for exoplanets. At this point, it seems clear that interferometry and AO are complementary, and neither can reach its full potential without the other. The fourth chapter introduces the origin and problem of imaging through atmospheric turbulence, and the limitations imposed by the atmosphere on the performance of speckle imaging. Further, it deals with the AO system including discussions of wavefront compensation devices, wavefront sensors, control system etc.

Interferometric technique bloomed during the last few decades. The new generation interferometry with phased arrays of multiple large sub-apertures would provide large collecting areas and high spatial resolution simultaneously. Over the next decades or so, one may envisage the development of hypertelescope (see Sect. 7.5.2). With forthcoming many-aperture systems, interferometry is indeed expected to approach the snapshot imaging performance of putative giant telescopes, the size of which may in principle reach hundreds of kilometers in space. However, daunting technological hurdles may come in the way for implementing these projects. Chapters 5–7 elucidate the current state-of-the art of such arrays. The various types of interferometric applications, for example, astrometry, nulling (see Sect. 5.1.3), and imaging are also described. These applications entail specific problems concerning the type of telescopes that are to be used, beam transportation and recombination, delay-lines, atmospheric dispersion, polarization, coherencing and cophasing, calibration, and detecting fringes using modern sensors (Chap. 6). Proposed ground and space-based interferometry projects (see Sects. 7.5–7.7) are also discussed.

Image-processing is an art and an important subject as well. A power spectrum (second-order moment) analysis provides only the modulus of the Fourier transform of the object, whereas a bispectrum (third-order moment) analysis (see Sect. 8.2.2) yields the phase reconstruction. The latter method is useful for simulations involving a diluted aperture interferometry. Indeed, it is difficult to incorporate adaptive optics system in a hypertelescope. Observations may be carried out by speckle interferometry, using either a redundant or non-redundant many-element aperture. Deconvolution method can also be applied to imaging covering the methods spanning from simple linear deconvolution algorithms to complex non-linear algorithms.

Chapter 8 discusses the methodology of recovering visibility functions of stellar diameter, ratio of brightness of binary components etc., from the raw data obtained by means of interferometry. Various image restoration techniques are also presented with emphasis on the deconvolution methods used in aperture-synthesis mapping.

Many astrophysical problems, such as measuring the diameters and asymmetries of single stars, observing stars as extended and irregular objects with magnetic or thermal spots, flattened or distorted by rapid rotation, determining the orbits of multiple stars, and monitoring mass ejections in various spectral features as they flow towards their binary companions, resolving star-formation regions, distant galaxies, AGNs, need high angular resolution information. Although a relatively new field, the steady progress of interferometry has enabled scientists to obtain results from the area of stellar angular diameters with implications for emergent fluxes, effective temperatures, luminosities and structure of the stellar atmosphere, dust and gas envelopes, binary star orbits with impact on cluster distances and stellar masses, relative sizes of emission-line stars and emission region, stellar rotation, limb-darkening, and astrometry. With the recent interferometers, Very Large Telescope Interferometer (VLTI) in particular, disks around several Young Stellar Objects (YSO), a few debris disks, core of a Luminous Blue Variable (LBV) object and a nova, several Active Galactic Nuclei (AGN) have been resolved. Some of these results obtained by means of optical/IR interferometry are enumerated in chapter nine. Also, it contains discussions on the ability of these instruments to obtain information about the accretion disks, winds and jets, and luminosities of components in binary systems.

I am grateful to A. Labeyrie and V. Trimble for their encouragement and indebted to G. Weigelt, O. Absil, D. Mourard, R. Millan-Gabet, Luc Damé, J. D. Monnier, A. Domiciano de Souza, F. Malbet, P. Lawson, P. M. Hinz, J. P. Lancelot, P. Nisenson, V. Chinnappan, V. Coudé du Foresto, T. R. Bedding, O. Lardière, P. Stee, Ishwara Chandra, P. Hoeflich, D. Soltau, S. LeBohec, A. Subramaniam, S. Golden, D. Braun, D. Bonneau, K. E. Rangarajan, and J. Buckley for providing the images, plots, figures etc., and granting permission for their reproduction. Special thanks are due to R. Ramesh, S. Morel, F. Sutaria, V. Valsan, T. Berkefeld, K. R. Subramaniam, T. P. Prabhu, C. S. Stalin, G. C. Anupama, A. Satya Narayanan, S. P. Bagare, and P. R. Vishwanath for going through selected chapters. I express gratitude for the services rendered by B. A. Varghese, S. Arun, V. K. Subramaniam, R. K. Chaudhuri, and D. Takir as well.

Swapan K. Saha

Principal Symbols

$a(\mathbf{r})$	Complex amplitude of the wave
$\mathbb{A}_e$	Effective area of an antenna
$\mathbf{B}$	Baseline vector
$B(\mathbf{u})$	Atmosphere transfer function
$B_\nu(T)$	Spectral radiancy
$\mathcal{B}_n(\mathbf{r})$	Covariance function
$\mathcal{C}_n^2$	Refractive index structure constant
$\mathcal{C}_T^2$	Temperature structure constant
$\mathcal{C}_v^2$	Velocity structure constant
D	Diameter of the aperture
$\mathcal{D}_n(\mathbf{r})$	Refractive index structure function
$\mathcal{D}_T(\mathbf{r})$	Temperature structure function
$\mathcal{D}_v(\mathbf{r})$	Velocity structure function
$G(\theta, \phi)$	Antenna gain
H_0	Hubble constant
I	Intensity of light
$\widehat{I}(\mathbf{u})$	Image spectrum
I_ν	Specific intensity
j	$= 1, 2, 3$
$J(\mathbf{r}_1, \mathbf{r}_2)$	Mutual intensity function
$\mathcal{J}_{12}$	Interference term
l	Characteristic size of viscous fluid
l_c	Coherence length
l_0	Inner scale length
$\mathcal{L}_\star$	Stellar luminosity
m_v	Apparent visual magnitude
M_v	Absolute visual magnitude

$M_\star$	Stellar mass
$n(\mathbf{r}, t)$	Refractive index of the atmosphere
$\widehat{N}(\mathbf{u})$	Noise spectrum
$O(\mathbf{x})$	Object illumination
$\widehat{O}(\mathbf{u})$	Object spectrum
P	Pressure
$P(\theta, \phi)$	Antenna power pattern
$P(\mathbf{x})$	Pupil transmission function
$\widehat{P}(\mathbf{u})$	Pupil transfer function
$\mathcal{R}$	Resolving power of an optical system
$\mathbf{r}(= x, y, z)$	Position vector of a point in space
R_e	Reynolds number
$\Re$ and $\Im$	Real and imaginary parts of the quantities in brackets
r_0	Fried's parameter
$R_\star$	Stellar radius
$\hat{\mathbf{s}}$	Unit vector
$S(\mathbf{x})$	Point Spread Function
$\langle \widehat{S}(\mathbf{u}) \rangle$	Transfer function for long-exposure image
$\mathcal{S}_r$	Strehl ratio
$\widehat{S}(\mathbf{u})$	Optical Transfer Function
t	Time
T	Period
$T_a(\theta, \phi)$	Antenna temperature
$T_b(\theta, \phi)$	Brightness temperature
$\mathbf{u}$	Spatial frequency vector
$U(\mathbf{r}, t)$	Complex representation of the analytical signal
$V(\mathbf{r}, t)$	Monochromatic optical wave
v_a	Average velocity of a viscous fluid
$\mathcal{V}$	Visibility
$\mathbf{x} = (x, y)$	Two-dimensional space vector
$\gamma(\mathbf{r}_1, \mathbf{r}_2, \tau)$	Complex degree of (mutual) coherence
$\Gamma(\mathbf{r}_1, \mathbf{r}_2, \tau)$	Mutual coherence
$\Gamma(\mathbf{r}, \tau)$	Self coherence
δ	Phase difference
ε	Energy dissipation
(θ, ϕ)	Polar coordinates
κ	Wave number
λ	Wavelength
λ_0	Wavelength in vacuum

$\mu(\mathbf{r}_1, \mathbf{r}_2)$	Complex coherence factor
ν	Frequency
$\Delta\nu$	Spectral width
$\langle\sigma\rangle$	Standard deviation
$\langle\sigma\rangle^2$	Variance
τ_0	Atmospheric coherence time
τ_c	Coherence time
$\Phi_n(\mathbf{k})$	Power spectral density
$\Delta\varphi$	Optical path difference
Ψ	Time-dependent wave-function
ω	Angular frequency
$*$	Complex operator
$\star$	Convolution operator
$\otimes$	Correlation
$\langle\ \rangle$	Ensemble average
$\widehat{\ }$	Fourier transform operator
$\boldsymbol{\nabla}$	Linear vector differential operator
∇^2	Laplacian operator

Some Numerical values of Physical and Astronomical Constants

c	Speed of light	3×10^8 m/s
G	Gravitational constant	6.674×10^{-11} N.m^2/kg^2
h	Planck's constant	6.626196×10^{-34}J.s
k_B	Boltzmann's constant	1.380662×10^{-23} J/K
$\mathcal{L}_\odot$	Solar luminosity	3.839×10^{26} W
$M_\odot$	Solar mass	1.9889×10^{30} kg
$R_\odot$	Solar radius	6.96×10^8 m
$T_\odot$	Solar effective temperature	5780° K
ϵ_0	Permittivity constant	8.8541×10^{-12} F/m
μ_0	Permeability constant	1.26×10^{-6} H/m
σ	Stefan–Boltzmann's constant	5.67×10^{-8}W m^{-2} K^{-4}

List of Acronyms

ACT	Atmospheric Cerenkov Telescope
AGB	Asymptotic Giant Branch
AGN	Active Galactic Nuclei
AMBER	Astronomical Multiple BEam Recombiner
BID	Blind Iterative Deconvolution
BLR	Broad-Line Region
CHARA	Center for High Angular Resolution Astronomy
CMBR	Cosmic Microwave Background Radiation
COAST	Cambridge Optical Aperture Synthesis Telescope
ESA	European Space Agency
ESO	European Southern Observatory
FLUOR	Fiber-Linked Unit for Optical Recombination
FINITO	Fringe-tracking Instrument of Nice and Torino
FSU	Fringe Sensor Unit
GI2T	Grand Interféromètre à deux Télescopes
GMRT	Giant Meterwave Radio Telescope
HR	Hertzsprung–Russell
HST	Hubble Space Telescope
IAU	International Astronomical Union
IMF	Initial Mass Function
IO	Integrated Optics
IOTA	Infrared Optical Telescope Array
IRAS	InfraRed Astronomical Satellite
ISI	Infrared Spatial Interferometer
ISM	InterStellar Medium
I2T	Interféromètre à deux Télescopes
IUE	International Ultraviolet Explorer
KT	Knox–Thomson
laser	Light Amplification by Stimulated Emission of Radiation
LBOI	Long Baseline Optical Interferometry

LBT	Large Binocular Telescope
IUE	International Ultraviolet Explorer
KT	Knox–Thomson
laser	Light Amplification by Stimulated Emission of Radiation
LBOI	Long Baseline Optical Interferometry
LBT	Large Binocular Telescope
LBV	Luminous Blue Variable
LD	Limb-Darkened
LIGO	Laser Interferometer Gravitational-Wave Observatory
LISA	Laser Interferometer Space Antenna
LPV	Long-Period Variables
mas	milliarcseconds
MCAO	Multi-Conjugate Adaptive Optics
MEM	Maximum Entropy Method
MIDI	MID-Infrared Interferometric Instrument
MMT	Multi Mirror Telescope
MROI	Magdalene Ridge Observatory Interferometer
MTF	Modulation Transfer Function
NASA	National Aeronautics and Space Administration
NLR	Narrow-Line Region
NPOI	Navy Prototype Optical Interferometer
NRAO	National Radio Astronomy Observatory
OPD	Optical Path Difference
OTF	Optical Transfer Function
OVLA	Optical Very Large Array
pc	Parsec
PMS	Pre-Main Sequence
PN	Planetary Nebula
PRIMA	Phase-Referenced Imaging & Microarcsecond Astrometry
PSF	Point Spread Function
PTI	Palomar Testbed Interferometer
PTF	Pupil Transmission Function
QUASAR	QUASi-stellAR radio source
RAFT	Real time Active Fringe Tracking
REGAIN	REcombineur pour GrAnd INterféromètre
SAO	Special Astrophysical Observatory
SIM	Space Interferometry Mission
SKA	Square Kilometer Array
SMBH	Super Massive Black Holes
SN	Supernova
SoHO	Solar and Heliospheric Observatory

SOIRDÉTÉ	Synthèse d'Ouverture en Infra Rouge avec DEux TElescopes
SUSI	Sydney University Stellar Interferometer
TC	Triple-Correlation
TPF	Terrestrial Planet Finder
UD	Uniform Disk
VBO	Vainu Bappu Observatory
VEGA	Visible spEctroGraph and polArimeter
VINCI	VLT INterferometer Commissioning Instrument
VLA	Very Large Array
VLBI	Very Long Baseline Interferometry
VLTI	Very Large Telescope Interferometer
VSI	VLTI Spectro-Imager
WR	Wolf–Rayet
YSO	Young Stellar Object

Contents